

Mechanical Robustness of FPA in a-Si Microbolometer with Fine Pitch

Hee Yeoun Kim*, Kyoung Min Kim*, Byeong Il Kim*, Won Soo Jang**, Tae Hyun Kim** and Tai Young Kang**

* National Nanofab Center (NNFC), Korea, hyeounkim@nnfc.com, kkm@nnfc.com, kbiset@nnfc.com
 **OCAS Co., Korea, wsjang@ocas.co.kr, tykang@ocas.co.kr

ABSTRACT

The microbolometer array sensor with fine pitch pixel array has been implemented to the released amorphous silicon supported by two contact pads. For the design of focal plane with geometrical flatness, the simple beam test structures were fabricated and characterized. As the beam length decreased, the effect of beam width on the bending was minimized. Membrane deformation of focal plane in a real pixel showed downward curvature by residual stress of a-Si and Ti layer. The tilting deformation was caused by the mis-align effect of contact pad and confirmed by FEA (Finite Element Analysis) simulation results. The electro-optical properties of bolometer have been measured as such that the NETD, 145 mK, the TCR, -2 %/K, and thermal time constant, 1.99 ms.

Keywords: microbolometer, amorphous silicon, IR sensor, residual stress

1 INTRODUCTION

Uncooled microbolometer has the various applications in many commercial and military applications. Among many sensor materials, amorphous Si have been widely used as sensor materials for their good TCR (Temperature Coefficient of Resistance), mechanical strength, low thermal mass and high manufacturing yield.[1] One of the advantages with uncooled microbolometer is the low cost achievable compared to cooled quantum detectors.[2-5] Low cost development has driven the pitch reduction approach. Obviously, owing to the increase of the number of dies per wafer, this will reduce the cost of the bolometer array itself with help of high manufacturing yield in a given processing defects density as well as the dimension of the bolometer packaging. [6]

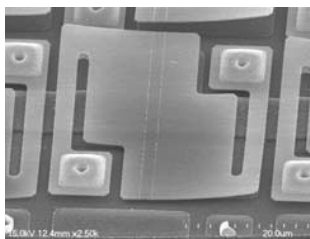


Figure 1. FPA showing upper curvature by the residual stress.

Currently, microbolometers with fine pitch have commercially developed by several foundries.[7,8] These developments aim at increasing the thermal insulation of the pixel and at reducing the $1/f$ noise. As shown in Fig. 1, such microbolometer FPA (Focal Plane Array) always have the curvature due to the intrinsic residual stresses in the dissimilar layers, leading to undesirable IR absorption useless. In this paper, we report an engineering approach to address this issue: the method we used includes a combination of test structure to analyze the simple beam geometry and FEA analysis of real pixel. In addition, the effects of misalign during fabrication process on mechanical robustness of FPA are investigated.

2 THEORETICAL BACKGROUND

Doubly supported beams with axial constraints at both ends can have net residual stresses due to thermal effects and these stresses can have profound effect on beam – bending behavior. The maximum deflection (w_{\max}) at the middle of the beam with uniform load (q) is as described as [9]

$$w_{\max} = \frac{L^4 q}{32EWH^3} \quad (1)$$

where L , E , W , H is length, elastic modulus, width and height of beam. In case of axial tension ($N = \sigma_0 WH$) in the beam, the maximum displacement is

$$w_{\max} = \frac{2qL}{4N} \left(\frac{L}{2} - 2 \frac{\cosh(k_0 L/2) - 1}{k_0 \sinh(k_0 L/2)} \right) \quad (2)$$

where k_0 is spring constant. For the case of compressive stress, the beam shows the buckling phenomena with maximum displacement of

$$w_{\max} = \sum_{n=1, \text{ odd}}^{\infty} \sqrt{\frac{2}{L}} \frac{2F}{EIk_n^4 + Nk_n^2} \quad (3)$$

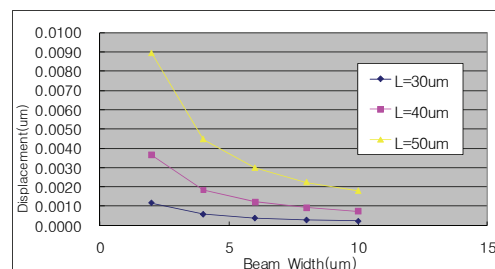


Figure 2. Maximum displacement of doubly supported beam with uniform loading, $q=100N$.

If we assume uniform loading, the beam deflection can be minimized when the beam length decreases and the beam width increases as shown in Figure 2. This result is analogous in the plane of a plate with bi-axial stress even though the mathematical analysis can get quite intricate.

3 EXPERIMENTAL METHODS

In order to investigate the mechanical robustness (bending and tilting) of FPA, two designs of simple beam and FPA are fabricated as shown in Figure 3. Microbolometer is composed of a thermometer integrated on a micro-bridge which is supported by two legs anchored over the ROIC (Read-out IC) wafer by metal studs. The micro-bridge and FPA have 0.3 μm thickness of doped amorphous silicon and 0.01 μm thickness of Ti layer and the gap between the mirror and the FPA is 2.0 μm . The simple beam structure to investigate the effect of beam geometry on residual stress is as shown in Figure 4. The beam length is ranged from 30 μm to 50 μm with 2, 4, 6, 8, 10 μm beam width. The beam length is defined as the distance between the released two supports.

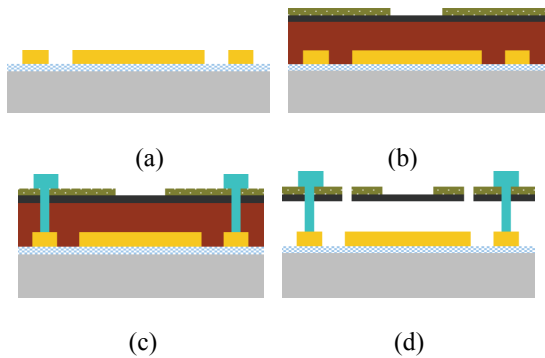


Figure 3. Fabrication process of a-Si microbolometer. (a) Electrode (mirror) patterning, (b) sacrificial layer, a-Si, Ti layer deposition, (c) contact pad formation, and (d) release

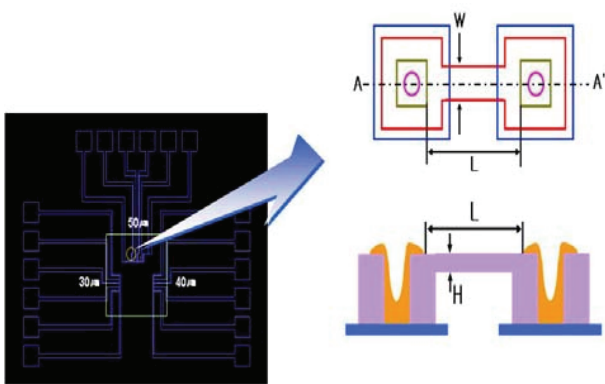


Figure 4. Design of doubly supported beam structure.

4 RESULTS AND DISCUSSIONS

4.1 Characterization of Doubly Supported Beams

Bending of doubly supported beams are measured by confocal optical profiler (Nanofocus AG). The effects of beam width on bending are minimized as the beam length decreased. Figure 5 shows similar trend to the analytical results of Figure 2.

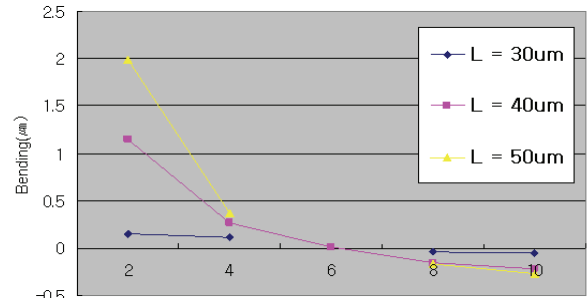


Figure 5. Variation of bending by length and width of fabricated beams

As the pixel pitch decreased, beam width and length connecting the contact pad and membrane (refer Figure 1) should be decreased at the same time. Therefore, it is confirmed that the effect of beam bending as the pixel pitch decreases is decreased.

4.2 Bending of Membrane Structure

Bending of real pixel with membrane structure is measured by same method and is shown in Figure 6. Membrane shows downward curvature. Its bending profile is different in horizontal and vertical direction so that the bending in horizontal direction (0.26 μm) is almost two times higher than that of vertical direction (0.12 μm).

Downward curvature of membrane is originated from the residual stress of a-Si and Ti layers consisting of membrane. The residual stress of a-Si and Ti are measured to 17MPa and -160MPa by laser curvature method. FEA results considering the residual stress of each layer show also downward curvature and the curvature of FPA is mainly controlled by thicker a-Si layer. Therefore, the residual stress has to be controlled to make the membrane structure with better flatness.

Tilted profiles of Figure 6 are not directly related to the residual stress of a-Si and Ti layer because the simulated profiles are symmetrical in horizontal and vertical directions as shown in Figure 7(b). Several parameters are simulated to figure out the origin of tilting of membrane structure. Figure 8 shows the simulation result showing the membrane bending profile as the contact pad location is shifted in specific direction (in our case, 1 μm in left and

upper direction) . Their tilting is 0.026um which is less than the experimental value.

It is presumed that the difference of experimental value and simulated value is caused by the exact description in the material property of contact pad. In real case of micromachining fabrication process, the overlay misalign error is normally occurred and the effect of misalign of contact pad location is important to determine the bending profile of FPA membrane structure.

In conclusion, mechanical robustness of FPA related to the IR absorbance can be implemented by optimization of residual stress and misalign accuracy of each layer consisting FPA.

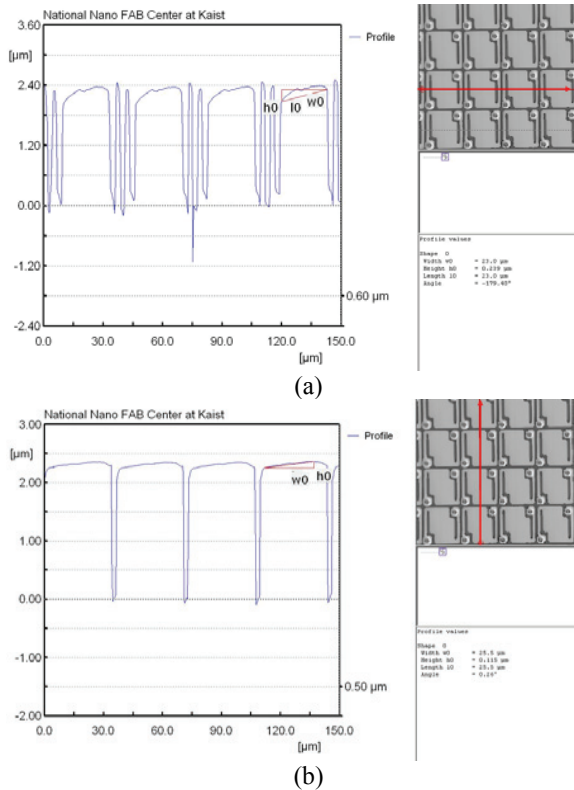


Figure 6. Bending profiles of membrane through (a) the horizontal and (b) vertical directions.

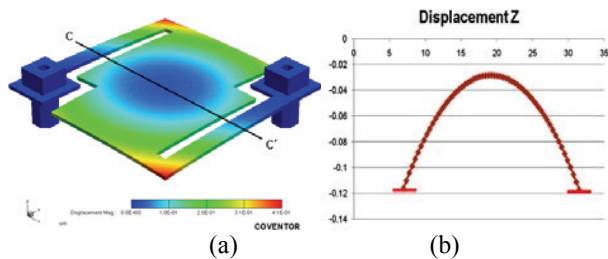


Figure 7. Simulation results showing the bending profile of unit pixel. (b) is the bending profile along C-C' line of (a).

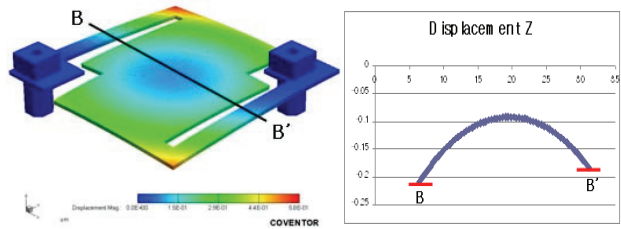


Figure 8. Simulation result showing the tilting of membrane due to the shift of contact pad location (1μm movement in left and upper direction)

4.3 Electro-optical Properties

Electrical properties of fabricated real pixels are measured by semiconductor characterization system (Keithley 4200 SCS). Figure 9 shows I-V curve of single pixel swept from -5V to +5V. It represents linear ohmic characteristics and the resistance is about 800kΩ at operating voltage.

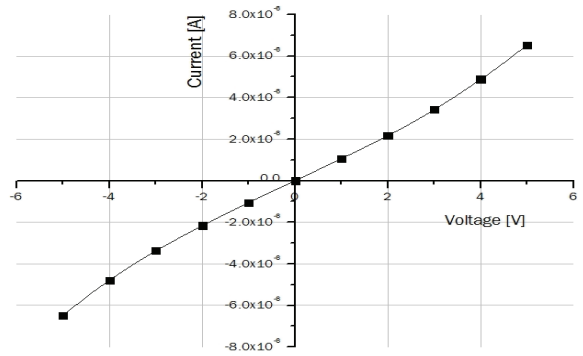


Figure 9. I-V curve of the element pixel

One of the most important figures of merit for microbolometer is NETD (Noise equivalent temperature difference) which is defined as the difference in temperature between two blackbodies of large lateral extent which gives rise to a difference in signal-to-noise-ratio of 1 in the electrical outputs of the two halves of the array, viewing the two blackbodies.

$$NETD = \frac{\Delta T}{SNR} = \frac{\Delta T}{V_{signal}} \cdot V_{noise} \quad (4)$$

Figure 10 shows the electrical output and noise obtained from the single pixel. Electrical output is measured to 21.05mV (V_{signal}) by the change of blackbody temperature from 60°C to 10°C (ΔT) and electrical noise (V_{noise}) beyond operating temperature range is 61μV. As a result, NETD is calculated to 145mK by eq. (6). Electrothermal properties are measured to the TCR of -2 %/K, and thermal time constant of 1.99 ms.

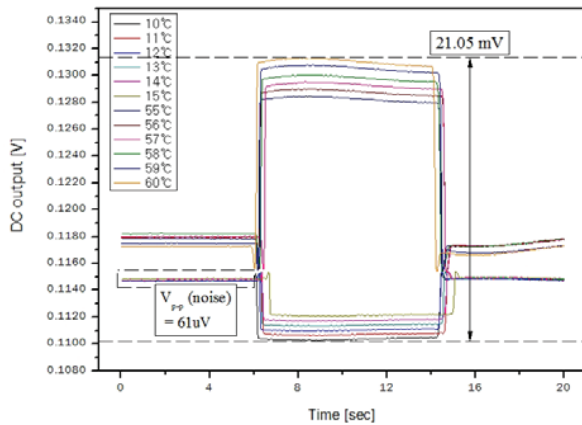


Figure 10. DC property of fabricated device by variation of blackbody temperature

5 CONCLUSION

Mechanical robustness of focal plane area is very important to maintain IR absorption performance as the microbolometer pixel size is decreased. In this paper, the doubly supported beam structures are designed and characterized to figure out the effect of geometry. The effects of beam width on beam bending are minimized as the beam length decreased and it shows similar trend to the analytical results. It is confirmed that the membrane structure of microbolometer FPA is little affected by the beam geometry because the width and length of beam connecting the contact pad and membrane is decreased as the pixel pitch decreased. Bending of membrane structure in real pixel is measured and it shows downward curvature and tilting deformation. Downward curvature of membrane is originated from the residual stress of a-Si and Ti layers consisting of membrane. FEA results show that the curvature of FPA is mainly controlled by thicker a-Si layer. Tilting deformation of membrane is related the shift of contact pad due to the mis-align. In conclusion, mechanical robustness of FPA related to the IR absorbance can be implemented by optimization of residual stress and align accuracy of each layer consisting FPA. By the optimization of fabrication process, we obtain FPA with good mechanical robustness. I-V curve of single pixel represents linear ohmic characteristics and the resistance is about 800k Ω at operating voltage and its NETD is calculated to 145mK.

REFERENCES

- [1] Yue Kuo, "Thin film Transistors", Kluwer Academic Publishers. 2003.
- [2] Y. Zhao, M. Mao, R. Horowitz, A. Majumdar, J. Varesi, P. Norton, and J. Kitching, "Optomechanical Uncooled Infrared Imaging System Design, Microfabrication and

Performance", *Journal of MEMS*, Vol 11, No. 2, April 2002.

- [3] E. L. Dereniak, and G. D. Boreman, *Infrared Detectors and Systems*, John Wiley&Sons, New York, 1996.
- [4] Kazuhiko Hashimoto, Huaping Xu, Tomonori Mukaigawa, Ryuichi Kubo, Hong Zhu, Minoru Noda, Masanori Okuyama, "Si monolithic microbolometers of ferroelectric BST thin film combined with readout FET for uncooled infrared image sensor", *Sensors and Actuators*, Vol 88, p.10-19, 2001.
- [5] Sabuncuoglu Tezcan, D., Eminoglu, S., Sevket Akar, O., "A low cost uncooled infrared microbolometer focal plane array using the CMOS n-well layer", *Micro Electro Mechanical Systems*, 14th IEEE Int MEMS Conference, p. 566-569, 2001
- [6] F. Niklaus, C. Vieider, H. Jakobsen, "MEMS-based uncooled infrared bolometer arrays: a review" *Proc. SPIE*, Volume 6836, p. 68360D, 2008.
- [7] J. L. Tissot, C. Trouilleau, B. Fieque, A. Crastes and O. Legras, "Uncooled microbolometer detector: recent developments at ULIS" *Opto-Electronics Review* 14(1) p.25-32, 2006.
- [8] R.A.Wood, "Uncooled thermal imaging with monolithic silicon focal planes" *Proc. SPIE*, Volume 2020, p. 322, 1993.
- [9] Stephen D. Senturia, "Microsystem Design", Kluwer Academic Publishers 2001.